Influence of Shear on Solvated Amphiphilic Block Copolymers with Lamellar Morphology

Johannes Zipfel,[†] Jörg Berghausen,[†,‡] Gudrun Schmidt,[†,§] Peter Lindner,[†] Paschalis Alexandridis,[||] and Walter Richtering*,[⊥]

Institut Laue-Langevin, B.P. 156, F-38042 Grenoble, France; Department of Chemical Engineering, University at Buffalo, The State University of New York, Buffalo, New York 14260-4200; and Institut für Physikalische Chemie, Christian-Albrechts-Universität zu Kiel, Olshausenstrasse 40, D-24098 Kiel, Germany

Received September 27, 2001

ABSTRACT: The effect of shear on lyotropic lamellar phases consisting of amphiphilic block copolymers was studied by in situ small-angle neutron scattering (SANS) and rheo-optics. Two different ternary systems containing a commercially available Pluronic type poly(ethylene oxide)-*b*-poly(propylene oxide)-*b*-poly(ethylene oxide) block copolymer, P123 ($EO_{20}PO_{70}EO_{20}$) or F127 ($EO_{100}PO_{70}EO_{100}$), as well as water and butanol were investigated over a wide range of concentrations. Orientation diagrams were constructed for both ternary systems; both exhibited a parallel-to-perpendicular transition of planar lamellae and a shear-induced formation of multilamellar vesicles (also termed liposomes, onions, or spherulites). For both systems, the vesicle formation occurred at low polymer content close to the phase boundary of the lamellar region and was accompanied by shear thickening. In addition, the kinetics and temperature dependence of the parallel-to-perpendicular transition were studied.

1. Introduction

Amphiphilic block copolymers exhibit a solution behavior similar to low molecular weight surfactants. They are known to segregate at the molecular level and associate into micelles when dissolved in a selective solvent.[1−3] Micelle formation, however, is only one facet of the rich phase behavior of such systems. At higher block copolymer concentrations and in the presence of a single selective solvent or two immiscible selective solvents, self-assembly can lead to a large variety of lyotropic liquid crystalline phases including lamellar, hexagonal-packed cylindrical micellar, cubic packed spherical micellar, and bicontinuous cubic structures.

In amphiphilic block copolymers, the chain length of the different blocks can be easily controlled by the polymerization process. For this reason, they offer great flexibility in setting the desired morphology and allow a larger variation of the length and time scales characteristic of the self-assembled structures as compared to typical surfactants.[4] An understanding of the principles which govern the self-assembly of solvated block copolymers not only is interesting from a fundamental point of view but also has important implications for modern materials science since amphiphilic block copolymers find numerous applications as foam stabilizers, thickeners, wetting agents and compatibilizers.[5] A special focus in recent research is placed on the use of self-assembled block copolymer structures in pharmaceutical and biomedical applications[6] and for the preparation of nanostructured materials like mesoporous ceramics.[7,8]

* To whom correspondence should be sent. E-mail: richtering@phc.uni-kiel.de.
[†] Institut Laue-Langevin.
[‡] Present address: Solvias AG, Basel, Switzerland.
[§] Present address: Department of Chemistry, Louisiana State University, Baton Rouge, Louisiana 70803-1804.
[||] University at Buffalo, The State University of New York.
[⊥] Christian-Albrechts-Universität zu Kiel.

The control of mesoscopic structure and orientation of self-assembled lyotropic systems is feasible by means of shear flows.[9,10] In many applications block copolymer solutions are subjected to flow fields (for example in detergent formulations or in drug delivery), and thus, it is of great interest to study the effect of flow on structure and orientation of such systems. So far, most of the studies have been performed on well-characterized systems,[11] e.g., lyotropic lamellar systems.[12] The behavior of lyotropic lamellar phases consisting of low molecular weight surfactants gained particular interest since the lamellae could not only be aligned or reoriented under shear[13−19] but also be transformed into a fascinating state of densely packed multilamellar vesicles, often called onions.[20−24] For recent reviews see, e.g., refs 11, 12, and 25.

In contrast to the large number of studies that have been performed on lamellar phases of low molecular weight surfactants and on block copolymer melts,[26−28] only a few studies addressed lamellar block copolymer solutions.[29−31] The layers in a lamellar block copolymer phase typically align with their normal either along the velocity gradient direction in the so-called *parallel* (or *c*) orientation or with the normal along the neutral direction in the *perpendicular* (or *a*) orientation.

Balsara and co-workers[29,30] studied the influence of shear on a concentrated block copolymer solution of a poly(styrene)−poly(isoprene) (SI) diblock in dioctylphthalate with small-angle neutron scattering (SANS) under shear. Below the order−disorder temperature (ODT) a transition from a *parallel* to a *perpendicular* orientation was observed by applying steady shear. This transition could also be observed using oscillatory shear by increasing the frequency at a fixed temperature.[32] A systematic difference in the defect density between parallel and perpendicular alignment was also noted.

Aqueous solutions of triblock copolymers of the type poly(ethylene oxide)−poly(propylene oxide)−poly(ethylene oxide) (PEO−PPO−PEO), also known as Pluronics

10.1021/ma0116912 CCC: $22.00
Published on Web 04/06/2002

or Poloxamers, were mostly studied since they are commercially available in a variety of molecular weights and block ratios. Mortensen studied the influence of shear on a lamellar phase of the Pluronic triblock copolymer P85 ($EO_{25}PO_{40}E_{25}$) and reported that parallel and perpendicular alignment coexist under shear with all other lamellar orientations in which layers are parallel to the flow direction.[13]

Our group studied lamellar solutions of Pluronic P123 ($EO_{20}PO_{70}EO_{20}$) and F127 ($EO_{100}PO_{70}EO_{100}$) in butanol/water mixtures.[33,34] These systems are unique since the lamellar region is formed at rather low block copolymer concentrations.,[35,36] For solutions with an intermediate block copolymer concentration, a *parallel-to-perpendicular* transition was observed. At lower polymer concentrations in the same system, a shear-induced formation of multilamellar vesicles (onions) was observed for the first time in a lamellar block copolymer system.[33] This structure is especially appealing for the encapsulation of active ingredients.[37]

Motivated by these results, the aim of the present work was to study the structural transitions of these two solvated Pluronic block copolymer systems in greater detail in order to construct orientation diagrams as previously published for low molecular weight surfactants.[20,23] Obviously, butanol plays a key role in these systems. It does not behave like typical oil but rather as a cosurfactant since it has some affinity to both PEO and PPO blocks of the copolymer.[38] Structural changes should hence be expected when the butanol-to-water ratio is changed at constant block copolymer concentration. The influence of the polymer concentration can be checked by keeping the butanol-to-water ratio constant.

We used SANS at the Bragg peak in order to monitor in situ structural changes under shear. With the Couette type shear geometry in SANS, it is possible to achieve two different beam configurations, the radial (where the beam is parallel to the shear gradient direction) and the tangential configuration (where the beam is along the flow direction). Kinetics of structural changes were investigated with time-resolved SANS.

The paper is organized as follows: we first describe the experimental techniques used in this study and give an overview on the sample compositions and the sample structure at rest. Then results on the influence of shear will be presented for both Pluronic systems and summarized in orientation diagrams. Finally, we will discuss the influence of different parameters (e.g., the polymer concentration, block length or the butanol-to-water ratio) on the behavior under shear and compare our results with the properties of lamellar block copolymer melts and surfactant−water mixtures under shear.

2. Experimental Section

Materials and Sample Preparation. The poly(ethylene oxide)-*b*-poly(propylene oxide)-*b*-poly(ethylene oxide) block copolymers, Pluronic P123 (PEO_{20}-*b*-PPO_{70}-*b*-PEO_{20}), and Pluronic F127 (PEO_{100}-*b*-PPO_{70}-*b*-PEO_{100}) were kindly supplied by BASF Corp. and used without further purification. The nominal weights of Pluronic P123 and Pluronic F127 are 5750 and 12600 and their EO contents are 30 and 70%, respectively. P123 and F127 have the same PPO middle block but different PEO end blocks. Butanol-1 was purchased from BDH Chemical Ltd (Poole, England) and used as received. The samples were prepared by weighing in appropriate amounts of block copolymer in D_2O and butanol into glass tubes. They were rigorously mixed and allowed to equilibrate for at least 1 week. All samples fell within the one-phase region of the isothermal phase diagrams.[35,36] The samples were transparent and birefringent and remained transparent under shear.

Small-Angle Neutron Scattering. All neutron scattering experiments have been performed on the instrument D11 at the Institut Max von Laue-Paul Langevin (ILL) in Grenoble, France. The neutron wavelength was 6 Å with a spread of $\Delta\lambda/\lambda = 9\%$. Static measurements were performed with 1 mm cuvettes (Hellma) covering a range of momentum transfer q from 3.5×10^{-3} to 0.44 $Å^{-1}$. The data were collected on a two-dimensional multidetector (64×64 elements of 1×1 cm^2) and corrected for background and empty cell scattering. The incoherent scattering of H_2O was used for absolute calibration according to standard procedures and software available at the ILL. Further analysis was done by radial averaging. Here, 20° sectors around the peak position were used in the analysis of anisotropic SANS spectra.

A Couette cell consisting of two quartz cylinders where the outer one rotated at controlled rate was used for measurements under shear. The gap was 1 mm, and a rectangular aperture of 0.3 mm × 15 mm was employed to reduce the beam size. Two scattering configurations were used. (i) The so-called radial position yields information in the plane formed by flow and vorticity direction. (ii) The tangential position probes structures in the plane of gradient and vorticity direction. The transmission of the neutron beam in radial and tangential beam configuration is very different due to the different beam size and path length. The radial beam data were calibrated to absolute units as mentioned above and provide the scattering intensity along flow and neutral (vorticity) direction. The latter direction is also probed in the tangential beam configuration and was used to shift the tangential beam data such that the intensity along the vorticity direction superposed with the radial beam data.

The SANS intensity for the surface plots is given in a linear scale (relative units), such that the scaling is identical for different SANS patterns of the same beam configuration. Radial and tangential data, however, are scaled differently due to the different transmissions.

The shearing time at a given shear rate was typically 10−15 min which is sufficient to reach steady state when vesicles are not involved. During the shear thickening transition of vesicle containing samples a steady state was not always reached at low shear rates.

Shear experiments were performed by controlling either the stress or the rate. The parallel-to-perpendicular transition is the same in both shear modes. Vesicle samples, however, revealed different behavior concerning the vesicle degradation in stress and rate-controlled experiments, respectively similar to what was observed in other systems.[21,23,39] A critical stress is needed to destroy the vesicles while the use of constant rate yields to a biphasic state. Because of experimental constraints caused by higher viscosities (Weissenberg effect), this effect could not be studied in such details as compared to previous studies.

For rheo-optical studies, a stress controlled Bohlin CVO rheometer equipped with a quartz glass cone/plane shear geometry was used as described previously.[34]

3. Results

SANS Measurements at Rest. The phase diagrams of the $EO_{20}PO_{70}EO_{20}$ (P123)/butanol/water and of the $EO_{100}PO_{70}EO_{100}$ (F127)/butanol/water ternary isothermal (25 °C) systems were published by Alexandridis and co-workers[35] and are reproduced here in Figure 1 to provide a better view of the phase behavior for the ensuing discussion of the shear-induced structural changes.

In the P123 system, the L_α-phase is formed along the copolymer−water binary axis and can swell to a varying extent with butanol. The lamellar phase covers a broad range from 20 up to 80 wt % copolymer concentration. Several samples were studied along different lines. In one series, the block copolymer concentration was varied

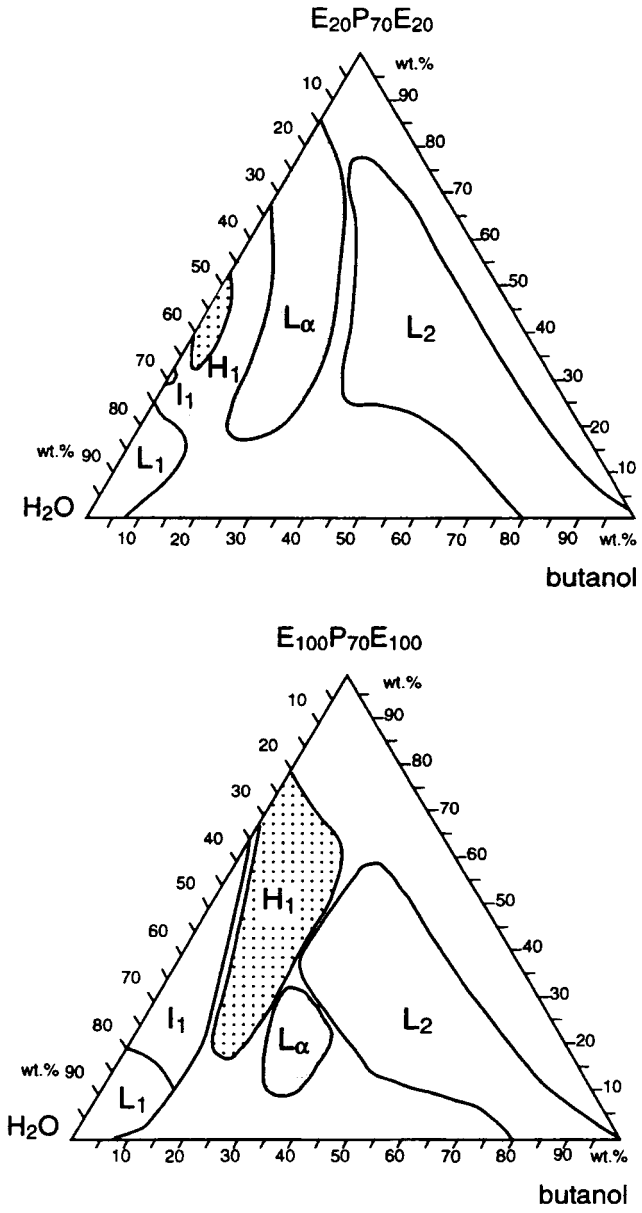

Figure 1. Phase diagrams of the PEO_{20}-*b*-PPO_{70}-*b*-PEO_{20} (Pluronic P123)/butanol/H_2O (top) and PEO_{100}-*b*-PPO_{70}-*b*-PEO_{100} (Pluronic F127)/butanol/H_2O (bottom) systems at T = 25 °C (modified from ref 35).

while the ratio of butanol to D_2O was fixed, while in a second series the block copolymer concentration was constant but the butanol-to-D_2O ratio was varied. Table 1 gives an overview of the samples studied at rest and under shear.

Figure 2 displays static SANS intensities from samples with a constant butanol-to-D_2O weight/weight ratio of 0.30, but different P123 block copolymer concentrations. The lamellar spacing decreases with increasing polymer concentration at a constant butanol content. Figure 3 displays SANS scattering curves of samples with a constant block copolymer concentration of 23% and a variation in the butanol-to-D_2O ratio from 0.30 to 0.50. With increasing butanol content, there is a decrease in lamellar spacing which is, however, small compared to the change when the polymer content was increased.

The $EO_{100}PO_{70}EO_{100}$ block copolymer is more hydrophilic than $EO_{20}PO_{70}EO_{20}$. It exhibits a lamellar phase at a low copolymer concentration but only when butanol is present, see Figure 1. Different samples have been studied parallel to the lines of the triangular phase diagram of the ternary system. Table 2 summarizes the composition and the lamellar spacing as revealed by SAXS. In principle, the same trends in lamellar spacing can be observed as for the $EO_{20}PO_{70}EO_{20}$ system. While the lamellar spacing increased with decreasing copolymer concentration, it was almost invariant to changes in the butanol/D_2O ratio at constant copolymer concentration.

Measurements Under Shear. The behavior of the P123 system was first studied along a dilution line with decreasing polymer content from 50% (w/w) to 18% (w/w) at a constant butanol/D_2O weight ratio of 0.30. The samples can be classified in three different categories as will be shown below:

- At high block copolymer content (above 30%), one can observe a shear-induced *parallel* orientation of lamellae.
- At low block copolymer content, the samples exhibit a reorientation transition from a *parallel* (*c*) to a *perpendicular* orientation (*a*) with increasing shear rate.
- At very low block copolymer content, a shear-induced *vesicle* formation is found.

SANS under shear is a powerful means to distinguish between the different types of layer orientations and structures under shear. The tangential beam is especially crucial since only in this beam configuration lamellae in the parallel orientation can be detected. Figure 4 shows the 3D-SANS patterns of the sample P11 (30/0.30) at two shear rates: 50 s^{-1} and 1200 s^{-1}, respectively. At low shear rates, a strong Bragg peak is observed along the velocity gradient direction with the tangential beam configuration. This clearly demonstrates that the bilayers were aligned parallel to the walls. The radial beam configuration only probes a very small amount of residual layers aligned perpendicularly. At higher shear rates, however, the layers reoriented with their normal along the neutral direction, as can be clearly seen from the results of the tangential and the radial beam experiment. In both configurations, Bragg scattering could be observed along the neutral direction. Thus, from SANS one can conclude that sample P11 (30/0.30) shows a reorientation from *parallel* (*c*) at low shear to *perpendicular* (*a*) at high shear rates.

Figure 5 displays the Bragg intensities in the three directions (flow, neutral, and gradient) along the dilution line (butanol/D_2O ratio = 0.3) for four different P123 block copolymer concentrations: 20%, 21%, 23%, and 30%, respectively. The samples with a 30% block copolymer concentration exhibited a transition from *parallel to perpendicular* at a shear rate of about 400 s^{-1}, whereas this transition was shifted to higher shear rates at a block copolymer concentration of 23%. At the highest accessible shear rate, the intensity along the neutral direction was higher than along the velocity gradient direction but the intensity ratio was not as high as for the 30% sample at this shear rate. Thus, the *parallel to perpendicular* transition was not completed for the 23% sample and both orientations coexisted. A coexistence of both orientations has been observed before and can be caused by a variation of layer orientation across the gap of the Couette shear cell as was observed by means of small-angle X-ray scattering from lamellar surfactant systems.[40]

The samples with the lowest block copolymer content did not show an orientation transition at all. Instead, a shear-induced formation of multilamellar vesicles (MLVs)

Table 1. Composition of the $EO_{20}PO_{70}EO_{20}$/Butanol/D_2O Samples and the Lamellar Spacing *D* (at 25 °C) As Revealed by SANS Measurements at Rest

sample	P123 (% w/w)	D_2O (% w/w)	butanol (% w/w)	BuOH/ D_2O (w/w)	D (Å)	shear-induced structures
P1 (18/0.3)	17.9	63.1	19	0.30	–	vesicles
P2 (20/0.3)	19.88	61.21	18.91	0.30	178	vesicles
P3 (21/0.3)	20.7	61.2	18.1	0.30	173	vesicles
P4 (21/0.35)	21.0	58.6	20.5	0.35	165	$c + a^{\{20\ s^{-1}\}}$vesicles
P5 (21/0.40)	21.0	56.5	22.5	0.40	161	*c*
P6 (23/0.30)	23.0	59.2	17.8	0.30	160	$c^{\{1500s^{-1}\}}a > c$
P7 (23/0.35)	22.9	57.1	20.0	0.35	154	$c^{\{40s^{-1}\}}$vesicles$^{\{1000s^{-1}\}}c$
P8 (23/0.40)	22.9	55.0	22.1	0.40	151	*c*
P9 (23/0.45)	22.8	53.1	24.1	0.45	149	*c*
P10 (23/0.50)	23.0	51.4	25.6	0.5	149	*c*
P11 (30/0.30)	30.0	53.8	16.2	0.30	139	$c^{\{800s^{-1}\}}a$
P12 (30/0.35)	30.0	51.9	18.2	0.35	135	*c*
P13 (30/0.40)	30.0	50.1	19.9	0.40	132	*c*
P14 (39/0.30)	38.71	47.11	14.18	0.30		*c*
P15 (50/0.30)	49.98	38.31	11.71	0.30	105	*c*

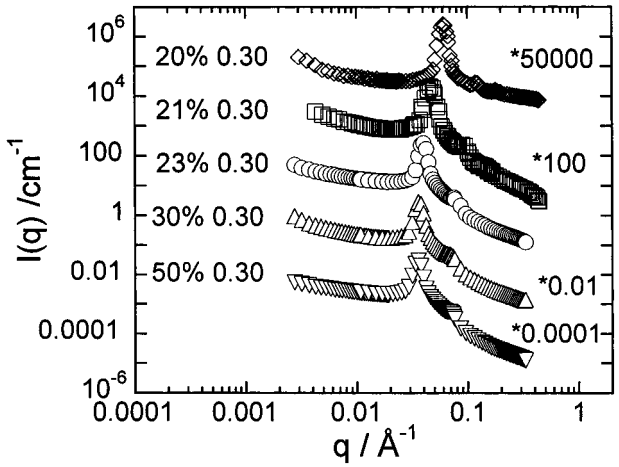

Figure 2. Static SANS intensity of $EO_{20}PO_{70}EO_{20}$ samples with a constant butanol-to-D_2O ratio of 0.30 and different copolymer concentrations.

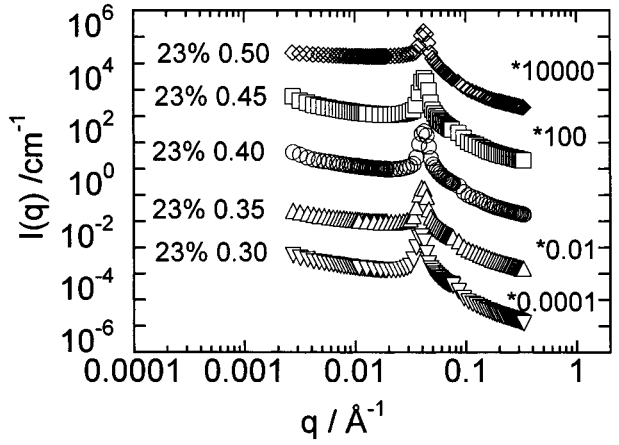

Figure 3. Static SANS intensity of $EO_{20}PO_{70}EO_{20}$ samples with an $EO_{20}PO_{70}EO_{20}$ concentration of 23% and different butanol-to-D_2O ratio.

was observed at 20% and 21% concentrations. The SANS intensity in the flow direction increased by a factor of ca. 10 for both samples as compared to the samples with higher polymer content that do not form MLVs. While the intensities along all three directions were on the same level for sample P2 (20/0.30), the intensity in neutral and gradient direction was higher than that in flow direction for sample P3 (21/0.30). This indicates that not all lamellae were transformed into multilamellar vesicles. Remaining lamellae orient most probably either in the parallel or perpendicular orientation but not in the transverse. For that reason, the intensity was lower in the flow direction where only the vesicles contribute to the scattering, as compared to the intensity in the other two directions. At high shear rates, the behavior was not clear for both samples. While a slight increase of the intensity in the gradient direction could be observed for sample P3 (21/0.30), sample P2 (20/0.30) could not be sheared at rates higher than 100 s^{-1} because the sample became heterogeneous apparently due to strong normal forces.

Table 2. Composition of the $E_{100}P_{70}E_{100}$/Butanol/D_2O and the Lamellar Spacing D (at 25 °C) As Revealed by SAXS Measurements at Rest

sample	F127 (%w/w)	D_2O (%w/w)	butanol (%w/w)	BuOH/ D_2O (w/w)	*D* (Å)	shear induced struct
F1 (12.5/0.67)	12.5	52.5	35.5	0.67	221	
F2 (12.5/0.58)	12.5	55.5	32.5	0.58	226	vesicles
F3 (12.5/0.52)	12.5	57.5	30	0.52	221	vesicles$^{\{1s^{-1}\}}c$
F4 (15.0/0.70)	15.0	50.0	35.0	0.70	189	$c^{\{300s^{-1}\}}a$
F5 (15.0/0.62)	15.0	52.5	32.5	0.62	189	vesicles$^{\{1s^{-1}\}}c$
F6 (15.0/0.55)	15.0	55.0	30.0	0.55	204	vesicles$^{\{1s^{-1}\}}c$
F7 (17.5/0.74)	17.5	47.5	35.5	0.74	185	
F8 (17.5/0.65)	17.5	50.0	32.5	0.65	181	
F9 (17.5/0.57)	17.5	52.5	30.0	0.57	177	c
F10 (20.0/0.78)	20.0	45.0	35.0	0.78	166	
F11 (20.0/0.68)	20.0	47.5	32.5	0.68	173	
F12 (20.0/0.60)	20.0	50.0	30.0	0.60	174	c
F13 (21.0/ 0.50)	21.0	52.5	26.3	0.50		$c^{\{1000s^{-1}\}}a > c$
F14 (22.5/0.63)	22.5	47.5	30.0	0.63		$c^{\{800s^{-1}\}}a >$ c
F15 (25.0/0.67)	25.0	45.0	30.0	0.67		$c^{\{1s^{-1}\}}a > c$

Figure 6 displays the SANS intensities in neutral, flow and gradient direction for the samples along a dilution line at butanol/D_2O = 0.35 (higher ratio than that in Figure 5. Three samples were studied, at block copolymer concentrations of 21% (P4), 23% (P7), and 30% (P12), respectively. Sample P12 exhibited a *parallel* orientation within the range of shear rates studied. At the highest shear rate accessible (1000 s^{-1}), the onset of a shear-induced reorientation could be observed. Sample P7 was in the *parallel* orientation at low shear rates as deducted from the high SANS intensity in the gradient direction. At a shear rate of 20 s^{-1}, the onset of the vesicle formation is revealed by the increase of intensity in the flow direction. At 40 s^{-1}, the intensity in the flow direction was maximum while the intensity in gradient direction was decreasing. At this shear rate, most of the lamellae were transformed to multilamellar vesicles. Figure 7 shows 3D SANS spectra obtained in the radial and tangential beam configuration from sample P7 in the vesicle state. The vesicles were stable

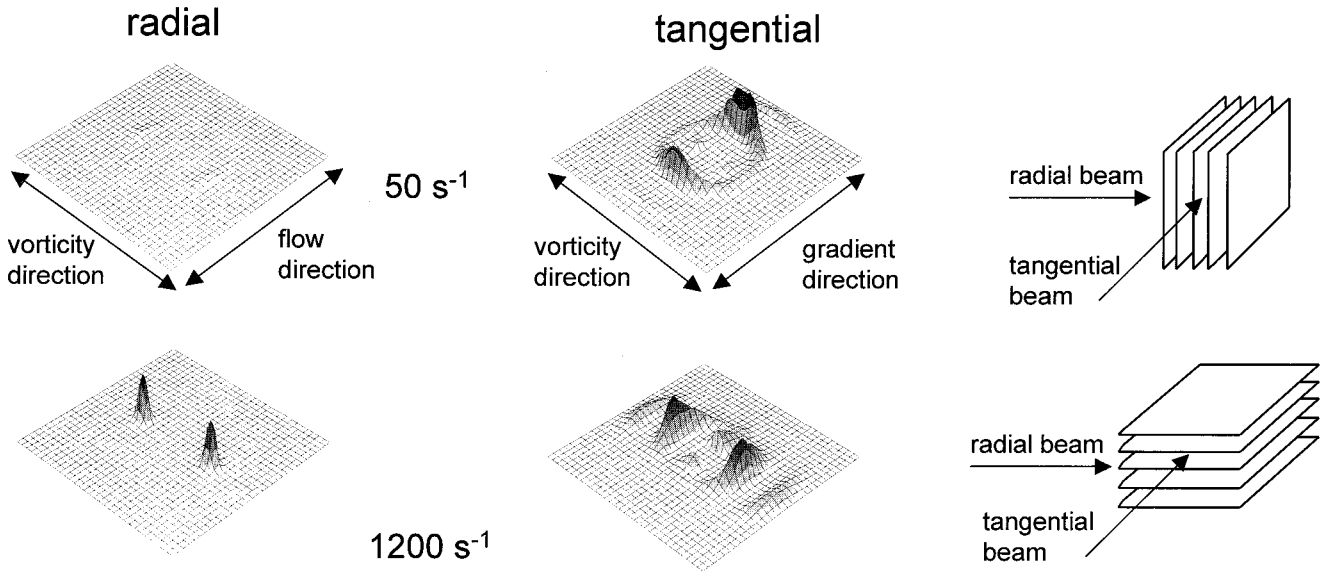

Figure 4. SANS patterns observed for the sample P11 (30/0.30) at shear rates of 50 (top) and 1200 s^{-1} (bottom): left, radial beam; right, tangential beam (different setting).

up to high shear rates, but above 1000 s^{-1} vesicle disruption was observed. There were no indications for a parallel to perpendicular transition for sample P7. Sample P4 showed similar behavior. At 20 s^{-1}, the vesicle formation was further developed than for sample P7 as can be seen in the higher intensity in flow direction. Disruption of the vesicles started at higher shear rates than 1000 s^{-1}, and no indication for a parallel to perpendicular transition of planar lamellae was observed. In depolarized small-angle light scattering a four-lobe pattern (four-leaf clover) was observed which is typical of multilamellar vesicles.[21,41] As a further illustration of vesicle samples, a polarized light micrograph of sample F2 showing Maltese crosses typical of vesicles is displayed in Figure 8.

Rheological Behavior. Figure 9 displays viscosity vs shear rate for P123 samples along the dilution line butanol/D_2O = 0.30. As described before, samples with copolymer concentrations of 20% and 21% formed vesicles which lead to high viscosity at low shear rates. As already mentioned in the Experimental Section, it is difficult to reach steady shear flow at low shear rates when vesicle formation occurs. Furthermore, the shear-induced vesicle formation is different when controlled shear rate and shear stress experiments are compared as was observed with low molar mass surfactants. Nevertheless, the typical feature of a viscosity maximum, which is caused first by the vesicle formation and then by a decrease in vesicle size, is reproducible.

The samples that displayed a *parallel to perpendicular* transition (25% and 30%) were shear thinning and had low viscosity when the *perpendicular* orientation was reached similar to the behavior of surfactant solutions. The viscosity of samples that prevailed in the *parallel* orientation (40% and 50%) was notably higher as compared to samples with a lower block copolymer concentration and the viscosity followed a power law $\eta \propto \dot{\gamma}^{-0.5}$ in the shear thinning regime.

P123 samples along a horizontal line with a constant block copolymer concentration of 23% revealed similar behavior. The viscosity of sample P7(23/0.35), which showed shear-induced vesicle formation, was about 1 order of magnitude higher as compared to the other samples. A viscosity maximum was observed for sample P7(23/0.35) similar to other samples showing shear-induced vesicle formation.

Influence of Temperature on the Parallel-to-Perpendicular Transition. The influence of temperature on the *parallel to perpendicular* transition was examined in the case of sample P11 (30/0.30) at two different temperatures: 25 and 30 °C. Figure 10 displays the SANS intensities along the three directions vs the shear rate. SANS intensity along the flow direction decreased with shear rate and did not significantly change with temperature. SANS intensities in gradient and vorticity direction showed similar effects up to shear rates of ca. 200 (25 °C) and 300 s^{-1} (30 °C), respectively. Critical shear rates, however, were temperature dependent. Above the critical shear rates a crossover point can be observed at 25 °C and 400 s^{-1} and at 30 °C and 1000 s^{-1}. At shear rates higher than 1000 s^{-1}, SANS intensities in gradient and vorticity direction have switched positions.

The *parallel* orientation of lamellae is more or less independent of rate and temperature at shear rates up to ca. 200 (25 °C) and ca. 300 s^{-1} (30 °C), respectively. Above the critical shear rate, the fraction of *parallel* oriented lamellae decreases and the fraction of *perpendicular* oriented lamellae increases while both orientations coexist. At the crossover point SANS intensities of both orientations are identical. The crossover point can be used to characterize the transition between parallel and perpendicular layer alignment and is sensitive to changes in temperature. At shear rates higher than 1000 s^{-1}, a perpendicular orientation of lamellae is well developed for 25 °C and dominates for 30 °C. One can conclude that the parallel-to-perpendicular transition is sensitive to changes in temperature and higher temperatures shift the transition to higher shear rates.

Kinetics of the Parallel-to-Perpendicular Transition. The kinetics of the *parallel to perpendicular* realignment was investigated with sample P11 by means of shear rate jump experiments. The sample was presheared at a shear rate of 50 s^{-1} for ca. 30 min in order to obtain a well-defined initial state. At this shear rate, the *parallel* orientation dominates. The shear rate was then suddenly increased to three different shear

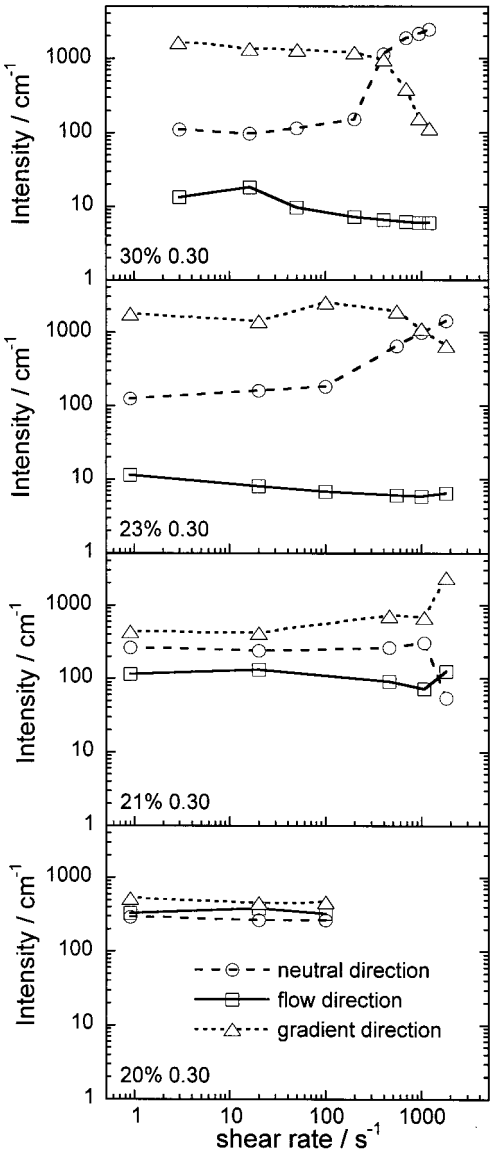

Figure 5. SANS intensities vs shear rate in neutral, flow and gradient direction for the samples P11(30/0.30), P6(23/0.30, P3 (21/0.30), and P2 (20/0.30) lines are to guide the eye.

rates: 400, 800, and 1200 s^{-1}, respectively. The evolution of the Bragg peak intensities in the radial beam experiment was followed with time-resolved SANS measurements. The transition for all three shear rates took place in less than 5−10 s (the recording time for one data point was 2 s). The plateau value for the SANS intensity in the neutral direction was identical for the two higher shear rates (800 and 1200 s^{-1}) while it was remarkably lower at 400 s^{-1}. At the latter shear rate, a major fraction of the lamellae were still in the parallel orientation. Another difference was that the fluctuation of the intensities lasted only about 10 s for the higher shear rates, while it took almost 30 s at the shear rate of 400 s^{-1}, until a steady state in the intensity was reached in the neutral direction. The intensities in the flow direction remained constant within experimental error. This indicates that the membranes prevailed intact during the transition, which is taking place in the neutral-shear gradient plane. The lower intensity along the neutral direction at the shear rate of 400 s^{-1} indicates a coexistence of parallel and perpendicular orientation, which was also observed in previous experiments. This indicates that the lamellae do not realign

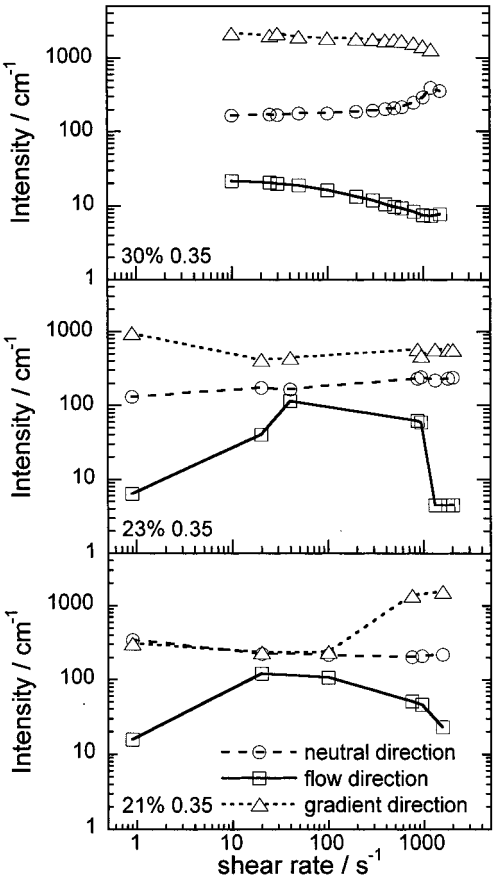

Figure 6. SANS intensities vs shear rate in neutral, flow and gradient direction for the samples P12 (30/0.35), P7 (23/0.35), and P4(21/0.35) lines are to guide the eye.

simultaneously, which is in agreement with experiments on surfactant lamellar phases; they revealed that the realignment starts at one wall of the shear cell.[40]

Orientation Diagrams. The influence of shear on the morphology of the various samples can be summarized with orientations diagrams, known from surfactant systems.[20,23] Figure 11 displays the structures that were obtained from $EO_{20}PO_{70}EO_{20}$ (P123) samples at a constant butanol/D_2O ratio of 0.3 and different polymer concentrations. Figure 12 also shows properties of the $EO_{20}PO_{70}EO_{20}$ (P123) system, but here polymer concentration is constant at 23% and the influence of the butanol/D_2O ratio can be seen.

Figure 13 provides an overview of the orientation behavior of all investigated $EO_{20}PO_{70}EO_{20}$ (P123)/butanol/D_2O samples. The samples are characterized by the block copolymer concentration and butanol/D_2O ratio and are marked with different symbols according to their behavior under shear. Samples, which aligned in the *parallel* orientation independent of the shear rate, are marked as squares whereas samples with a *parallel to perpendicular* transition have a triangle as symbol. Finally, samples which exhibited a formation of shear-induced lamellar vesicles are marked as circles.

At high polymer concentrations neither a shear-induced vesicle formation nor a parallel to perpendicular transition could be observed under the conditions examined. The *parallel to perpendicular* transition was detected at a constant butanol/D_2O ratio of 0.30 within a certain range of block copolymer concentration (between 25 and 30%). At a higher or lower concentration close to this concentration range, the transition appar-

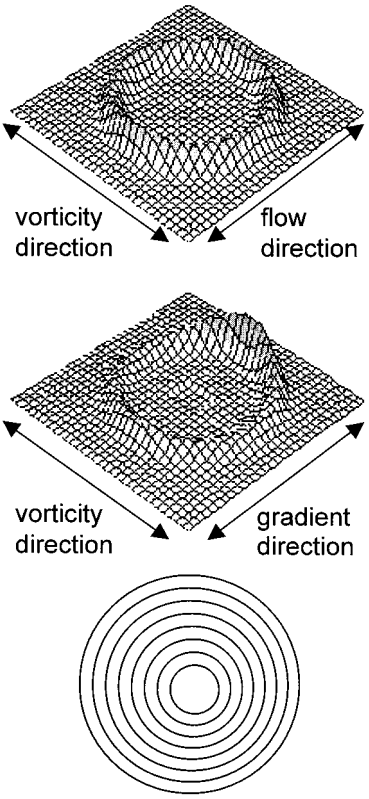

Figure 7. SANS patterns from sample P7 (23/0.35) in the vesicle state. radial (top) and tangential beam (bottom) at a shear rate of 40 s^{-1}.

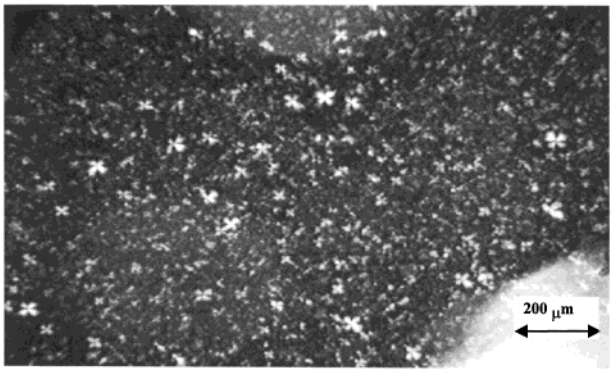

Figure 8. Polarization micrograph of sample F2 after shearing.

ently shifted to higher shear rates and thus could not be observed. For one sample (23%/0.30), the onset of this transition could be detected at the higher shear rates examined. Changing the butanol/D_2O ratio to the butanol rich side had the same effect on the parallel to perpendicular transition as a change in copolymer concentration. At a butanol/D_2O ratio of 0.35 no transition could be detected until 1000 s^{-1}. It is notable that the shift of the butanol/D_2O ratio from 0.30 to 0.35 at a polymer concentration of 30% had the same effect as an increase in temperature from 25 to 30 °C at a constant butanol/D_2O ratio of 0.30.

The formation of shear-induced multilamellar vesicles occurred without exception at very low block copolymer concentrations. The onset of vesicle formation depends on the butanol/D_2O ratio. At a butanol/D_2O ratio of 0.30 vesicle formation started immediately and no parallel orientation could be detected at very low shear rates. At a higher ratio of 0.35, vesicles were formed at shear

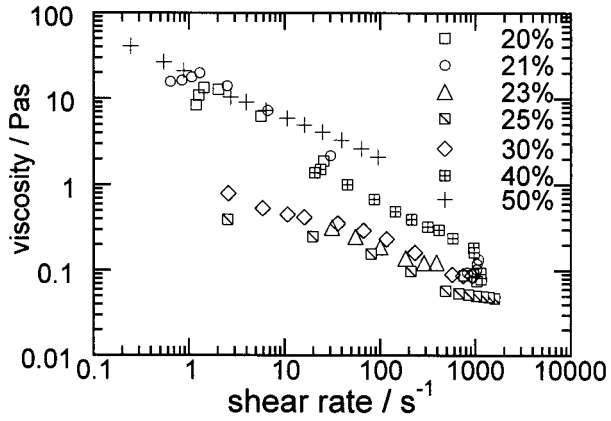

Figure 9. Viscosity vs shear rate for P123 samples along the dilution line butanol/D_2O = 0.30.

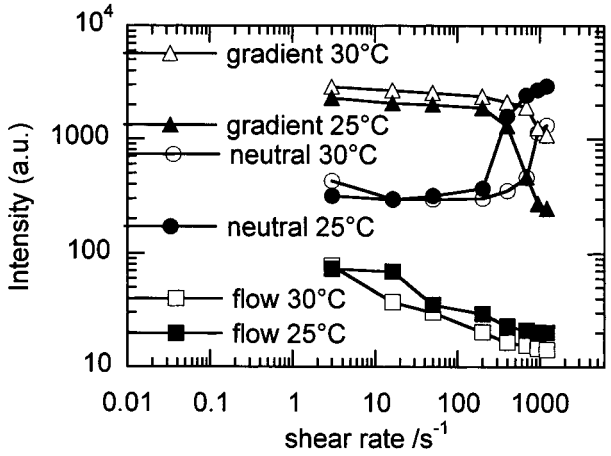

Figure 10. SANS intensities vs shear rate in neutral, flow, and gradient direction for the sample P11 (30/0.30). The solid symbols show the results at 25 °C; the open symbols show those at 30 °C.

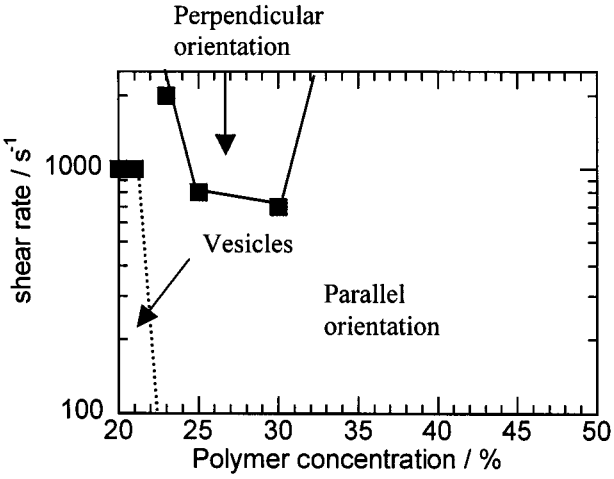

Figure 11. Orientation diagram of $EO_{20}PO_{70}EO_{20}$/butanol/D_2O at a butanol/D_2O ratio of 0.3: shear-induced structure vs polymer concentration.

rates of about 20 s^{-1}. The lamellae were not fully transformed into vesicles at this ratio and the viscosity was lower than that at lower butanol content. In addition to this, it was easier to destroy the vesicles at high shear rates than at a butanol/D_2O ratio of 0.30. At the polymer concentration of 23% only the sample with a butanol/D_2O ratio of 0.35 could be transformed into vesicles.

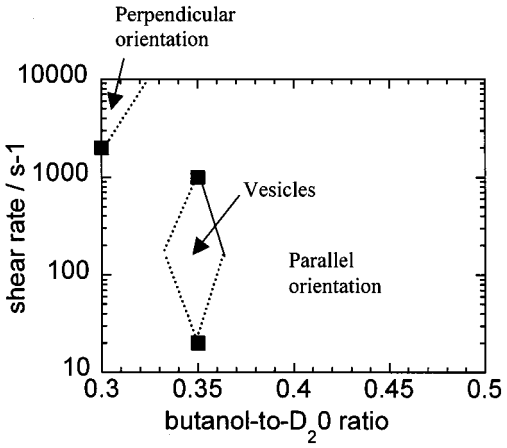

Figure 12. Orientation diagram of $EO_{20}PO_{70}EO_{20}$/butanol/D_2O at a polymer content of 23%: shear-induced structure vs butanol/D_2O ratio.

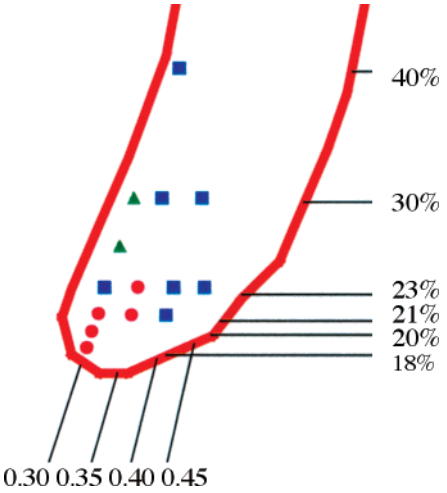

Figure 13. Orientation diagram of $EO_{20}PO_{70}EO_{20}$/butanol/D_2O The samples are characterized by the block copolymer concentration (to the left) and by the butanol/D_2O ratio (at the bottom). Samples with a parallel orientation within the range of shear rates available, have a square as symbol, samples with a parallel to perpendicular transition a triangle and samples with shear-induced formation of multilamellar vesicles a circle. The complete phase diagram is shown in Figure 1 (top).

Figure 14 displays the general orientation diagram of the system $EO_{100}PO_{70}EO_{100}$ (F127)/butanol/D_2O. Again samples are marked according to their behavior under shear. Samples that aligned in the *parallel* orientation independent of shear rate are marked with squares whereas samples with a *parallel to perpendicular* transition have a triangle as symbol. Samples which exhibited a formation of shear-induced lamellar vesicles, are marked as circles. Vesicles were only formed at very low block copolymer concentrations and at the butanol poor edge of the lamellar region in the phase diagram. The "vesicle island" in the $EO_{100}PO_{70}EO_{100}$ system is located at a similar part of the lamellar region as it was the case for the $EO_{30}PO_{70}EO_{30}$ system. The *parallel to perpendicular* transition, however, occurred at different regions in the phase diagram. At a F127 block copolymer concentration of 15%, a *parallel to perpendicular* transition could be observed on the butanol rich side of the phase diagram. Samples that exhibit only a parallel orientation are located at intermediate block copolymer concentrations (17.5−20%).

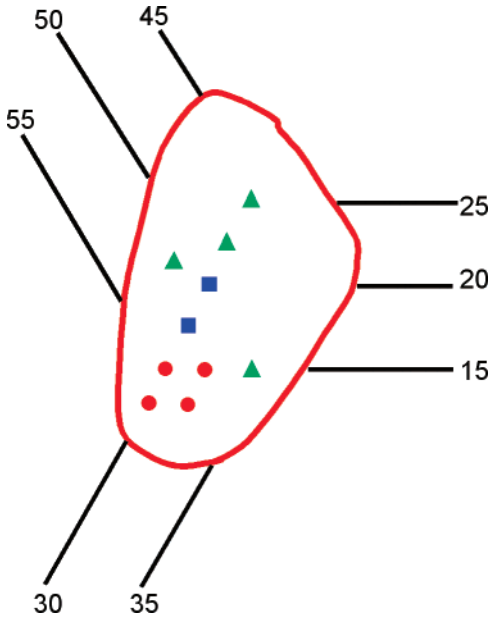

Figure 14. Orientation diagram of $EO_{100}PO_{70}EO_{100}$/butanol/D_2O. The samples are characterized by the block copolymer concentration (to the right), by the butanol concentration (at the bottom), and by the D_2O concentration (at the top). Samples with a parallel orientation within the range of shear rates available, have a square as symbol, samples with a parallel to perpendicular transition a triangle and samples with shear-induced formation of multilamellar vesicles a circle. The complete phase diagram is shown in Figure 1 (bottom).

4. Discussion

The ternary systems consisting of P123 (or F127)/butanol/D_2O exhibit an interesting and diversified behavior under shear. At the beginning of this discussion, however, the special role of butanol in the ternary systems and its possible impact on shear-induced structures should be mentioned.

Studies of Alexandridis and co-workers[35,36] revealed that butanol behaves more like a cosurfactant than an oil and thus cooperates with the block copolymer in forming the interface separating aqueous from oily domains. They found by SAXS measurements that the thickness of the apolar domain was considerably lower with butanol as compared to more hydrophobic solvents at identical water and block copolymer concentrations. With increasing butanol content, the apolar thickness of the lamellae decreased while it rose when the content of a more hydrophobic solvent like butyl acetate or xylene was increased. They confirmed these results with additional deuterium NMR measurements. The quadrupole splitting is proportional to the average hydration number of the copolymer, the order parameter of bound water molecules and the amphiphile/water molar ratio according to a conventional two-site model.[42] At a constant copolymer-to-water ratio, a decrease in the quadrupole splitting could be observed with increasing butanol concentration while an increase in the quadrupole splitting was observed with increasing butyl acetate concentration. The interfacially active butanol molecules can insert in the interfacial region and displace bound water molecules and thus decrease the hydration while the more hydrophobic butyl acetate molecules push out water into hydrophilic regions and thus increase the hydration. The role of alcohols in PEP−PPO−PEO block copolymer water systems and their location in the assemblies have been investigated

recently using SANS conditions where the deuteration of water and alcohol was varied.[43]

Alexandridis and co-workers concluded[35] that butanol is interfacial active, and the apolar volume fraction consists of PPO and only about 20% of the butanol volume fraction. Using this assumption, one can easily calculate the volume fraction of polar (PEO, D_2O and 80% butanol) and apolar (PPO and 20% butanol) parts of the ternary mixtures. With the apolar volume fraction f and the lamellar spacing D one can then calculate the apolar thickness δ of the membrane as $\delta = fD$. A table containing volume fraction, polar and apolar fractions, and the apolar thickness of the membranes of all samples is displayed in the appendix. Relevant trends will be discussed in the following. The two block copolymers differ in the length of the hydrophilic part. While P123 contains 30% (w/w) PEO, the fraction of PEO in F127 is 70%. Thus, the P123 system gets more hydrophobic with increasing block copolymer concentration as can be seen in the increasing fraction of apolar parts as listed in the appendix. For F127, this change in hydrophobicity is much smaller because this polymer has a more hydrophilic character. Since F127 is still more hydrophobic than the remaining components water and butanol, an increasing F127 concentration leads only to a slight increase in hydrophobicity.

A decrease in lamellar spacing was observed with increasing copolymer concentration indicating that the number of lamellae increased in order to accommodate the increasing number of copolymer molecules. At constant block copolymer concentration the spacing slightly decreased with increasing butanol content. This can be explained by the fact that an increasing butanol content at constant block copolymer concentration changes the apolar fraction only marginally since 80% of the butanol is located in the interface.

The conformation of the block copolymers in the lamellae could also have an impact on the behavior under shears. In principle, two conformations are conceivable: in the looplike conformation both hydrophilic ends are located at the same side with respect to the apolar domain while in the so-called bridging conformation the polymer is spanning through the apolar domain so that the two end segments are located on each side of the apolar domain. Theoretical considerations by Linse and co-workers[44] anticipate that the fraction of loops is related to the apolar thickness of the membranes. An increased thickness of the apolar domain would make it less likely for a block copolymer to span the apolar domain and thus will increase the probability to find both end segments on the same side of the apolar domain is reasonable. The domain spacing and the thickness of the apolar domain may also be varied by changing the temperature at a fixed ternary composition. A temperature increase results in a decrease in solubility of PEO and PPO in water,[45] leading to less hydrated PEO blocks and thus to a smaller interfacial area per copolymer. Both the apolar thickness and the fraction of loops are expected to rise with increasing temperature.

Studies on lyotropic lamellar phases of low molecular weight surfactants revealed that the viscoelastic properties of the surfactant bilayer play an important role for the structure under shear. Leon et al. investigated an ionic surfactant system in which the variation of salt concentration influences the saddle-splay modulus which could be correlated to the shear-induced formation of multilamellar vesicles.[46] Le et al. studied the influence of temperature in the planar lamellae to vesicle transition of a nonionic surfactant and found a correlation with the saddle-splay modulus.[47,48] The influence of water-soluble polymer on shear-induced vesicle formation of surfactant lamellar phases was studied by Berghausen et al., who discussed a correlation between the membrane properties characterized with the Caillé parameter and the MLV formation.[49] Undulation instabilities and texture defects are further parameters that influence the shear alignment of liquid crystals.[50−52] Recently Dhez et al. discussed the relevance of screw-like defects on the parallel to perpendicular transition of planar layers as well as on the vesicle formation.[53] Although the general behavior of surfactant lamellar phases under shear can be understood in terms of membrane properties and defect structures, small changes in the equilibrium properties can induce different structural transitions which makes it extremely difficult to predict which structure is the most favorable under steady shear.

Different parameters have also been discussed in the cases of block copolymer melts with lamellar morphology.[26−28,54] The undulation instability as well as selective melting and migration of defects have been discussed in order to explain the parallel to perpendicular transition in polymer melts similar to aqueous surfactant solutions as mentioned above.[27,55,56] Obviously, the viscoelastic contrast between the two polymer layers play an important role as well.[58] This viscoelastic contrast and the entanglements of macromolecules are specific parameters that influence shear alignment which, however, distinguish lamellar block copolymer melts from aqueous surfactant solutions.

The behavior of the solvated block copolymers under shear will now be discussed according to the experimental and theoretical considerations described above. Since shear-induced *vesicle* formation and *parallel-to-perpendicular* transitions occurred at different compositions these features will be discussed independently.

Shear-induced *vesicle* formation occurred for both systems at a very low block copolymer concentration and on the butanol poor side of the lamellar phase. Rather small changes in the composition can have an enormous influence on the rheological behavior. This can be seen, e.g., for the P123 system at a constant block copolymer concentration of 21%. The butanol/D_2O ratio was varied from 0.30 to 0.40. This leads to a change in the apolar volume fraction (PPO and 20% butanol) from 0.19 to 0.20 and to a decrease in the lamellar spacing from 173 to 161 Å. The apolar thickness of the membranes varies from 32.3 to 31.7 Å. In contrast to these minor differences in the samples' static properties, the behavior under shear was extremely different. While the sample with the lowest butanol/D_2O ratio of 0.30 exhibited a shear-induced vesicle formation at the lowest shear rates experimentally accessible, the vesicle formation started at shear rates of ca. 20 s^{-1} at a butanol/D_2O ratio of 0.35. At a butanol/D_2O ratio of 0.40, vesicle formation could not be observed at all.

Compared to the P123 system, vesicle formation in the F127 system could only be observed at extremely low shear rates. In addition, the vesicles could easily be destroyed by higher shear rates. The F127 polymer is more hydrophilic than P123 and its molecular weight is higher. To elucidate whether the composition of the polymer or the molecular weight is more important for

Table 3. Volume Fractions, Apolar Volume Fraction *f*, and Thickness of the Apolar Fraction *δ* for the P123/ Butanol/D_2O System

sample	PEO vol frac	PPO vol frac	butanol vol frac	D_2O vol frac	*D* (Å)	*f*(apolar) vol frac	*δ* (Å)
P1 (18/0.3)	0.053	0.122	0.241	0.585		0.170	
P2 (20/0.3)	0.059	0.135	0.239	0.567	177.5	0.183	32.43
P3 (21/0.3)	0.062	0.141	0.230	0.568	173.1	0.187	32.31
P4 (21/0.35)	0.062	0.141	0.258	0.539	164.9	0.193	31.83
P5 (21/0.40)	0.062	0.141	0.281	0.517	161.1	0.197	31.72
P6 (23/0.30)	0.069	0.156	0.226	0.549	159.5	0.202	32.14
P7 (23/0.35)	0.068	0.155	0.252	0.526	154.4	0.205	31.63
P8 (23/0.40)	0.067	0.153	0.276	0.503	150.7	0.209	31.45
P9 (23/0.45)	0.067	0.152	0.299	0.482	149.3	0.212	31.59
P10 (23/0.50)	0.067	0.152	0.316	0.465	149.1	0.216	32.14
P11 (30/0.30)	0.090	0.204	0.206	0.500	139.1	0.246	34.15
P12 (30/0.35)	0.089	0.203	0.229	0.479	135.1	0.249	33.60
P13 (30/0.40)	0.089	0.202	0.250	0.460	131.7	0.252	33.15
P14 (39/0.30)	0.116	0.264	0.181	0.439		0.300	
P15 (50/0.30)	0.150	0.342	0.150	0.358	104.7	0.372	38.96

Table 4. Volume Fractions, Apolar Volume Fraction *f*, and Thickness of the Apolar Fraction *δ* for the F127/ Butanol/D_2O System

sample	PEO vol frac	PPO vol frac	butanol vol frac	D_2O vol frac	*D* (Å)	*f*(apolar) vol frac	*δ* (Å)
F1 (12.5/0.67)	0.080	0.036	0.425	0.460	221	0.121	26.76
F2 (12.5/0.58)	0.080	0.036	0.393	0.491	226	0.115	25.99
F3 (12.5/0.52)	0.081	0.037	0.367	0.515	221	0.110	24.39
F4 (15.0/0.70)	0.096	0.044	0.421	0.440	189	0.128	24.14
F5 (15.0/0.62)	0.097	0.044	0.394	0.466	189	0.123	23.19
F6 (15.0/0.55)	0.098	0.044	0.367	0.492	204	0.118	23.99
F7 (17.5/0.74)	0.111	0.050	0.424	0.415	185	0.135	25.02
F8 (17.5/0.65)	0.113	0.051	0.394	0.443	181	0.130	23.51
F9 (17.5/0.57)	0.114	0.052	0.366	0.469	177	0.125	22.10
F10 (20.0/0.78)	0.128	0.058	0.420	0.395	166	0.142	23.56
F11 (20.0/0.68)	0.129	0.058	0.393	0.420	173	0.137	23.70
F12 (20.0/0.60)	0.130	0.059	0.366	0.446	174	0.132	22.98
F13 (21.0/0.50)	0.138	0.063	0.325	0.475		0.128	
F14 (22.5/0.63)	0.146	0.066	0.365	0.423		0.139	
F15 (25.0/0.67)	0.162	0.073	0.365	0.401		0.146	

the rheological behavior, one should check the rheological properties of a block copolymer consisting of equal amounts of PEO and PPO and a similar molecular weight. For such studies the block copolymer P105 $(EO)_{37}(PO)_{58}(EO)_{37}$ could be suitable; however, this material was not available for use in our present investigation. In a second step, one should investigate block copolymers with equal PEO/PPO ratios but different molecular weights.

There was no sample where both a vesicle formation *and* a parallel-to-perpendicular transition could be observed. The following trends could be observed for the P123 system: A *parallel to perpendicular* transition was only observable in the range 25−30% block copolymer concentration. For samples with a constant block copolymer concentration, the transition was shifted to higher shear rates with increasing butanol content. In agreement with this finding, a temperature increase shifted the *parallel to perpendicular* transition to higher shear rates. As stated above, a temperature increase results in a decrease of the solubility of PEO and PPO in water and thus reduces the degree of hydration and the interfacial area per block copolymer and increases the apolar thickness of the membranes.

As mentioned above, butanol can be considered as a cosurfactant and consequently one can discuss a series of samples with constant water content but varying surfactant (i.e. block copolymer)/cosurfactant (butanol) ratio. From Figure 13, one can see that the general trend for the P123 system is as follows: parallel-to-perpendicular transition at low butanol content; vesicles at intermediate and parallel alignment at high butanol content. This trend is very similar to what was observed in the surfactant system sodium dodecyl sulfate/decanol/water when the surfactant cosurfactant ratio was changed.[23]

With surfactants, it is well-known that the surfactant/cosurfactant ratio strongly influences the viscoelastic properties of the membrane[59] and thus influences the behavior under shear. In analogy, we suggest that butanol acts as cosurfactant in the present case and similar to classical surfactant systems small changes in the composition can lead to very different behavior under shear.

Comparing the results presented in this work to the influence of shear on block copolymer melts and on lyotropic lamellar phases consisting of low molecular weight surfactants leads to the conclusion that amphiphilic block copolymers in these ternary systems resemble more the latter. Apparently the membranes in amphiphilic block copolymers resemble very much the flexible membranes of lyotropic liquid crystals. During a shear-induced vesicle formation, a deformation of the membranes occurs which seems to be rather difficult for systems with membranes like those in block copolymer melts. The fact that vesicles are only formed at extremely low block copolymer concentrations underlines this hypothesis.

The *parallel-to-perpendicular* transition is common to all membrane systems, block copolymers and surfactants. It seems to be a general feature of lamellar systems under shear and might be correlated rather to macroscopic properties like bulk viscosity and texture defects than to molecular properties of the membrane.

5. Conclusions

The studies on the ternary systems consisting of PEO−PPO−PEO type block copolymers, butanol and water showed a diversified behavior under shear. Butanol acts rather as cosurfactant than as oil in such systems since it is interfacially active. At very low block copolymer concentrations and in the butanol poor edge of the lamellar region, a shear-induced formation of *multilamellar vesicles* was observed. While the MLVs in the P123 system were extremely viscous and persistent to higher shear rates, the vesicles were easily degraded in the F127 system. Small changes in the composition, which were almost imperceptible from static SANS experiments, had an enormous impact on the rheological behavior indicating a delicate balance of forces. Apparently the viscoelastic properties of the membrane are very sensitive to compositional changes similar to common surfactant bilayers. At intermediate block copolymer concentrations, the *parallel* orientation prevailed independent of the shear rate. At higher block copolymer concentrations a *parallel-to-perpendicular* orientation was observed. This transition was shifted to higher shear rates with increasing temperature, block copolymer concentration and butanol content.

It is obvious that the combination of shear flow and molecular composition in solvated block copolymers offers tremendous possibilities to influence the microscopic structure as well as the mesoscopic morphology. Many applications, e.g., in encapsulation and materials synthesis, can be envisioned and need to be explored.

Acknowledgment. We thank the Deutsche Forschungsgemeinschaft and the Fonds der Chemischen

Industrie for financial support as well as the Deutscher Akademischer Austauschdienst and the Svenska Institut for a travel grant. J.Z. acknowledges a Marie-Curie fellowship of the European Union. P.A. thanks the U.S. National Science Foundation (Grant CTS-9875848) for partial support of this research.

Appendix: Volume Fractions of the Block Copolymer Samples

To calculate the volume fractions of polar and apolar parts of the ternary systems consisting of P123/F127−butanol−D_2O, the following parameters were used:

	P123	F127	butanol	D_2O
density (g/cm^3)	1.05	1.05	0.81	1.11
molar mass (g/mol)	5750	12600	74.12	20.03

Given the molecular volume of one PEO group (72.4 Å^3) and one PPO group (95.4 Å^3), one can calculate the volume fraction of PEO and PPO in P123 and F127. The volume fraction of PEO is 0.31 in P123 and 0.69 in F127, respectively. The polar volume fraction is considered to consist of PEO, D_2O, and 80% of the butanol, while the apolar volume fraction f consists of PPO and 20% butanol. The thickness δ of the apolar volume fraction f can be calculated as $\delta = fD$.

Table 3 displays the volume fractions for the ternary P123/butanol/D_2O system, the apolar volume fraction f and the thickness of the apolar fraction δ. Table 4 contains the corresponding data for the F127/butanol/D_2O system.

References and Notes

(1) Tuzar, Z.; Kratochvil, P: in *Surface and Colloid Science*; Matjevicm, E.; Ed.; Plenum Press: New York, 1993; Vol. 15.
(2) Alexandridis, P.; Hatton, T. A. In *The Polymeric materials Encyclopedia*; Salamone, J. C., Ed; CRC Press: Boca Raton, FL, 1996; p 743.
(3) Bates, F. S.; Maurer, W. W.; Lipic, P. M.; Hillmyer M. A.; Almdal, K.; Mortensen, K.; Fredrickson G. H.; Lode T. P. *Phys. Rev. Lett.* **1997**, *79*, 849.
(4) Alexandridis, P.; Olsson, U.; Lindman, B. *Langmuir* **1998**, *14*, 2627.
(5) Edens, M. W. In *Nonionic Surfactants: Polyoxyalkylene Block Copolymers*; Nace, V. M., Ed.: Marcel Dekker Inc.: New York, 1996.
(6) Yang, L.; Alexandridis, P. In *Controlled Drug Delivery*; Park, K., Mrsny, R. J., Eds.; ACS Symposium Series 752; American Chemical Society: Washington, DC, 2000; pp 364−374.
(7) Foerster, S.; Antonietti, M. *Adv. Mater.* **1998**, *10*, 195.
(8) Feng, P.; Bu, X.; Pine D. J. *Langmuir* **2000**, *16*, 5304−5310.
(9) *Structure and Flow in Surfactant Solution*; Herb, C. A., Prudíhomme, R. K., Eds.; ACS Symposium Series 578; American Chemical Society: Washington, DC, 1994.
(10) *Flow-Induced Structures in Polymers*; Nakatani, A. I., Dadmun, M. D., Eds.; ACS Symposium Series 597; American Chemical Society: Washington, DC, 1995.
(11) Hamley, I. W. *Curr. Opin. Colloid Interface Sci.* **2001**, *5*, 342.
(12) Mortensen, K. *Curr. Opin. Colloid Interface Sci.* **2001**, *6*, 140.
(13) Mortensen, K. *J. Phys.: Condens. Matter* **1996**, *8*, A103.
(14) Mortensen, K.; Talmon, Y.; Gao B.; Kops, J. *Macromolecules* **1997**, *30*, 6764.
(15) Pople, J. A.; Hamley, I. W.; Fairclough, J. P. A.; Ryan, A. J.; Hill, G.; Price, C. *Polymer* **1999**, *40*, 5709.
(16) Mang, J. T.; Kumar, S.; Hammouda, B. *Europhys. Lett.* **1994**, *28*, 489.
(17) Penfold, J.; Staples, E.; Khan Lodhi, A.; Tucker, I.; Tiddy, G. J. T. *J. Phys. Chem. B* **1997**, *101*, 66.
(18) Berghausen, J.; Zipfel, J.; Lindner, P.; Richtering, W. *Europhys. Lett.* **1998**, *43*, 683.
(19) Mahjoub, H. F.; Bourgaux, C.; Sergot, P.; Kleman, M. *Phys. Rev. Lett.*, **1998**, *82*, 2076.
(20) Diat, O.; Nallet, F.; Roux, D. *J. Phys. II* **1993**, *3*, 1427.
(21) Bergenholtz, J.; Wagner, N. *Langmuir* **1996**, *12*, 3122.
(22) Bergmeier, M.; Gradzielski, M.; Hoffmann, H.; Mortensen, K. *J. Phys. Chem. B* **1999**, *103*, 1605.
(23) Zipfel, J.; Berghausen, J.; Lindner, P.; Richtering, W. *J. Phys. Chem. B* **1999**, *103*, 2841.
(24) Müller, S.; Börschig, C.; Gronski, W.; Schmidt, C.; Roux, D. *Langmuir* **1999**, *15*, 7558.
(25) Richtering, W. *Curr. Opin. Colloid Interface Sci.* **2001**, *6*, 446.
(26) Fredrickson, G. H.; Bates, F. S. *Annu. Rev. Mater. Sci.* **1996**, *26*, 501.
(27) Chen, Z.-R.; Kornfield, J. A.; Smith, S. D.; Grothaus, J. T.; Satkowski, M. M. *Science* **1997**, *277*, 1248.
(28) Wiesner, U. *Macromol. Chem. Phys.***1997**, *198*, 3319.
(29) Balsara, N. P.; Hammouda, B.; *Phys. Rev. Lett.* **1994**, *72*, 360.
(30) Balsara, N. P.; Hammouda, B.; Kesani, P. K.; Jonnalagadda, S. V.; Straty, G. C.; *Macromolecules* **1994**, *27*, 2566.
(31) Zyrd, J. L.; Burghardt, W. R. *Macromolecules*, **1998**, *31*, 3656.
(32) Wang, H.; Kesani, P. K.; Balsara, N. P.; Hammouda, B. *Macromolecules* **1997**, *30*, 982.
(33) Zipfel. J.; Lindner, P.; Tsianou, M.; Alexandridis, P.; Richtering, W. *Langmuir* **1999**, *15*, 2599.
(34) Zipfel. J.; Berghausen, J.; Schmidt, G.; Lindner, P.; Alexandridis, P.; Tsianou, M.; Richtering, W. *Phys. Chem. Chem. Phys.* **1999**, *1*, 3905.
(35) Holmqvist, P.; Alexandridis, P.; Lindman, B. *J. Phys. Chem. B.* **1998**, *102*, 1149.
(36) Holmqvist, P.; Alexandridis, P.; Lindman, B. *Macromolecules.* **1997**, *30*, 6788.
(37) A. Bernheim-Grosswasser, S. Ugazio, F. Gauffre, O. Viratelle, P. Mahy, D. Roux, *J. Chem. Phys.*, **2000**, *112*, 3424.
(38) Ivanova, R.; Lindman, B.; Alexandridis, P. *Langmuir* **2000**, *16*, 9058.
(39) Schmidt, G.; Müller, S.; Schmidt, C.; Richtering, W. *Rheol. Acta* **1999**, *38*, 486.
(40) Berghausen, J.; Zipfel, J.; Diat, O.; Narayanan, T.; Richtering, W. *Phys. Chem. Chem. Phys.* **2000**, *2*, 3623.
(41) Weigel, R.; Läuger, J.; Richtering, W.; Lindner, P. *J. Phys. II (Fr.)* **1996**, *6*, 529.
(42) Wennerström, H.; Lindman, B.; Lindblom, G. *Chem. Scr.* **1974**, *6*, 97.
(43) Alexandridis, P.; Yang, L. *Macromolecules* **2000**, *33*, 5574.
(44) Svensson, M.; Alexandridis, P.; Linse, P. *Macromolecules* **1999**, *32*, 5435.
(45) Goldmints, I.; von Gottberg, F. K.; Smith, K. A.; Hatton, T. A. *Langmuir* **1997**, *13*, 3659.
(46) Leon, A.; Bonn, D.; Meunier, J.; Al-Kahwaji, A.; Greffier, O.; Kellay, H. *Phys. Rev. Lett.* **2000**, *84*, 1335.
(47) Le, T.; Olsson, U.; Mortensen, K. *Phys. Chem. Chem. Phys.* **2001**, *3*, 1310.
(48) Le, T.; Olsson, U.; Mortensen, K.; Zipfel. J.; Richtering, W. *Langmuir* **2001**, *17*, 999.
(49) Berghausen, J.; Zipfel, J.; Lindner, P.; Richtering, W. *J. Phys. Chem. B* **2001**, *105*, 11081.
(50) Zilman, A. G.; Granek, R. *Eur. Phys. J. B* **1999**, *11*, 593.
(51) Auernhammer, G. K.; Brand, H. R.; Pleiner, H. *Rheol. Acta* **2000**, *39*, 215.
(52) Mayer, C.; Asnacious, S.; Bourgaux, C.; Kleman, M. *Rheol. Acta* **2000**, *39*, 223.
(53) Dhez, O.; Nallet, F.; Diat, O. *Eur. Phys. Lett.* **2001**, *55*, 821.
(54) Chen, Z.-R.; Kornfield, J. A. *Polymer* **1998**, *39*, 4679.
(55) Goulian, M.; Milner, S. T. *Phys. Rev. Lett.* **1995**, *74*, 1775.
(56) Winey, K. I.; Patel, S. S.; Larson, R. G.; Watanabe, H. *Macromolecules*, **1993**, *26*, 2542.
(57) Reference deleted in proof.
(58) Patel, S. S.; Larson, R. G.; Winey, K. I.; Watanabe, H. *Macromolecules*, **1995**, *28*, 4313.
(59) Boltenhagen, P.; Kleman, M.; Lavrentovich, O. P.; *J. Phys. II* **1994**, *4*, 1439.

MA0116912